ACS chemical biology

LETTERS

pubs.acs.org/acschemicalbiology

Structure Determination and Interception of Biosynthetic Intermediates for the Plantazolicin Class of Highly Discriminating Antibiotics

Katie J. Molohon,[†] Joel O. Melby,[‡] Jaeheon Lee,[§] Bradley S. Evans,[§] Kyle L. Dunbar,[‡] Stefanie B. Bumpus,[‡] Neil L. Kelleher,[⊥] and Douglas A. Mitchell[†,‡,§,*]

[†]Department of Microbiology, [‡]Department of Chemistry, and [§]Institute for Genomic Biology, University of Illinois at Urbana−Champaign, Urbana, Illinois 61801, United States

[⊥]Department of Chemistry and Chemistry of Life Processes Institute, Northwestern University, Evanston, Illinois 60208, United States

Supporting Information

ABSTRACT: The soil-dwelling, plant growth-promoting bacterium *Bacillus amyloliquefaciens* FZB42 is a prolific producer of complex natural products. Recently, a new FZB42 metabolite, plantazolicin (PZN), has been described as a member of the growing thiazole/oxazole-modified microcin (TOMM) family. TOMMs are biosynthesized from inactive, ribosomal peptides and undergo a series of cyclodehydrations, dehydrogenations, and other modifications to become bioactive natural products. Using high-resolution mass spectrometry, chemoselective modification, genetic interruptions, and other spectroscopic tools, we have determined the molecular structure of PZN. In addition to two conjugated polyazole moieties, the amino-terminus of PZN has been modified to N^{α},N^{α}-dimethyl-arginine. PZN exhibited a highly selective antibiotic activity toward *Bacillus anthracis*, but no other tested human pathogen. By altering oxygenation levels during fermentation, PZN analogues were produced that bear variability in their heterocycle content, which yielded insight into the order of biosynthetic events. Lastly, genome-mining has revealed the existence of four additional PZN-like biosynthetic gene clusters. Given their structural uniqueness and intriguing antimicrobial specificity, the PZN class of antibiotics may hold pharmacological value.

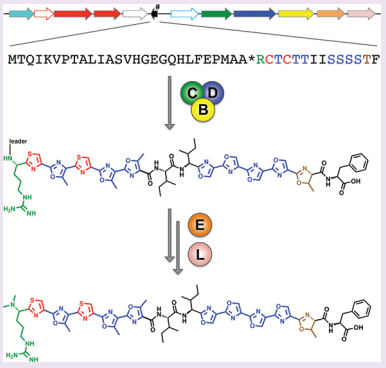

With facile access to low-cost next-generation DNA sequencing technology, there has been a recent surge in genome sequencing. The availability of nearly 2,000 microbial genomes has rekindled interest in the biosynthetic capabilities of bacteria.[1−4] Given the status of natural products and their derivatives as the largest source of all medicines, exploring uncharted biosynthetic territory holds vast potential.[5] One such region of natural product space includes the thiazole/oxazole-modified microcin (TOMM) family.[6−8] Unlike the well-known nonribosomal peptides and polyketides, TOMMs are derived from inactive, ribosomally synthesized precursor peptides. Each TOMM precursor peptide harbors an N-terminal leader region that serves as the binding site for enzymes that posttranslationally modify a C-terminal core region.[9,10] The distinguishing chemical features of a TOMM are heterocycles that derive from Cys, Ser, and Thr residues, which are abundant in the core region of the precursor peptide. During processing by a genetically conserved cyclodehydratase, select Cys and Ser/Thr amino acids undergo peptide backbone cyclization to become thiazoline and (methyl)oxazoline heterocycles. A subset of these are further subjected to a flavin mononucleotide (FMN)-dependent dehydrogenation, which yields the aromatic thiazole and (methyl)oxazole heterocycles. The formation of heterocycles on TOMM precursor peptides is dependent on the presence of a third component, termed the docking protein, whose exact function remains enigmatic.[11−13] Together, the TOMM cyclodehydratase (C), dehydrogenase (B), and docking protein (D) comprise a functional, heterotrimeric thiazole/oxazole synthetase. The genes encoding for this synthetase are typically located as adjacent open reading frames in bacterial genomes, making such biosynthetic clusters relatively easy to identify using routine bioinformatic methods.[7,14,15] TOMM biosynthetic clusters often contain ancillary tailoring enzymes that increase the chemical complexity of this natural product family.

Although the unification of the TOMM family of natural products has only recently emerged, the molecular structure and biological function of some TOMMs have long been established. Examples include microcin B17 (DNA gyrase inhibitor), the cyanobactins (eukaryotic cytotoxins), streptolysin S (disease-promoting cytolysin), and the thiopeptides (ribosome inhibitors).[3] As reported in early 2011, a plant growth-promoting bacterium, *Bacillus amyloliquefaciens* FZB42, produces a TOMM with antimicrobial activity toward select Gram-positive bacteria.[8] In this work, we report the structure and antimicrobial specificity of a TOMM natural product from FZB42. In addition to the natural production of PZN variants by FZB42, we discovered that other Gram-positive bacteria also contain PZN biosynthetic

Received: June 29, 2011
Accepted: September 27, 2011
Published: September 27, 2011

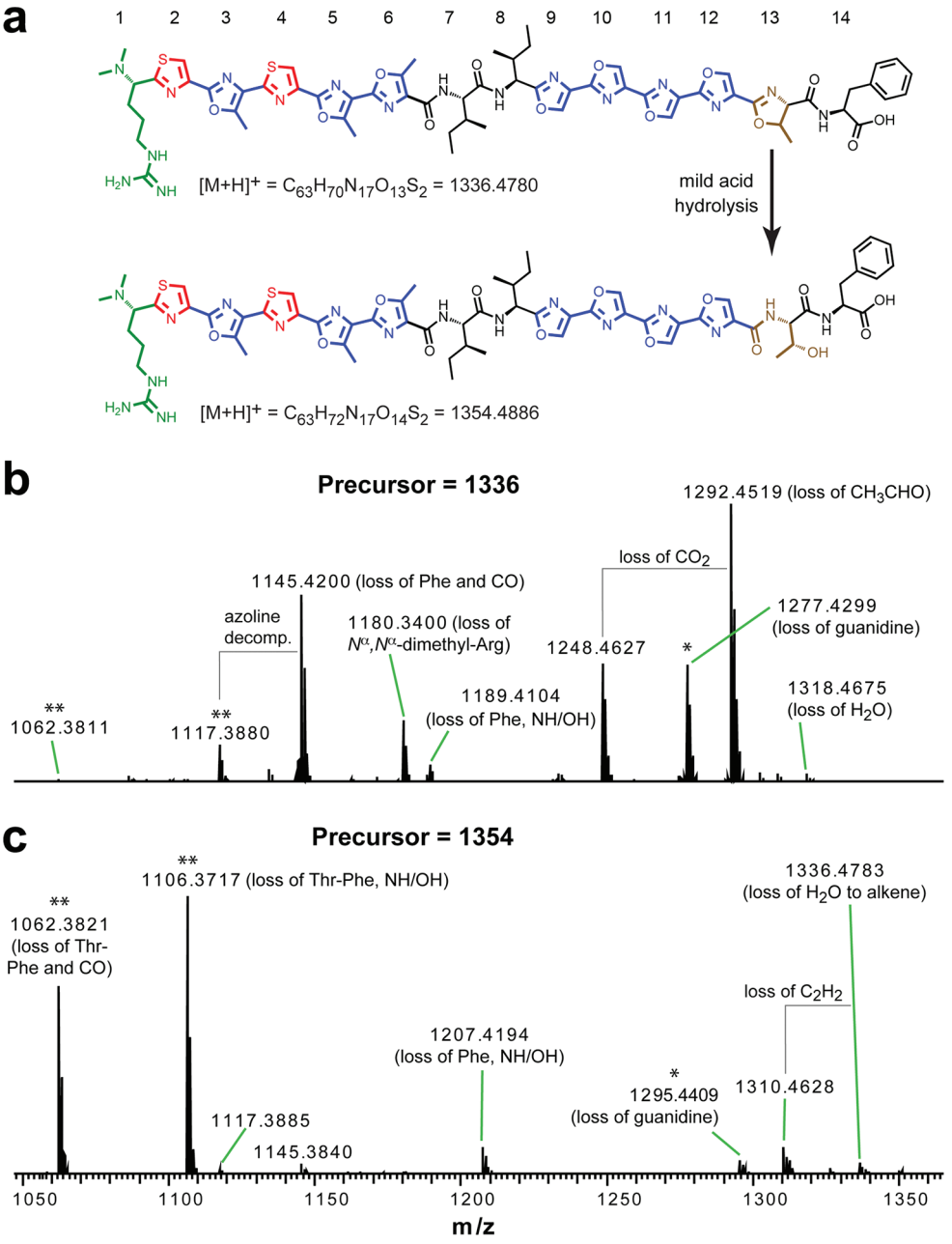

Figure 1. Mass spectrometry based structural elucidation of PZN. (a) After biosynthetic processing, the chemical structure of PZN features N^{α},N^{α}-dimethylArg (green), two thiazoles (red), seven (methyl)oxazoles (blue), and one methyloxazoline (brown). The numbering scheme used for each original residue is given at the top of the figure. After treatment with mild acid, azolines undergo hydrolytic ring opening to the original amino acid (in this case, Thr). (b) CID spectrum of the singly charged PZN ion (m/z 1336) acquired by LTQ-FT-MS. (c) Same as panel b, except the parental ion analyzed was hydrolyzed PZN (m/z 1354). *Denotes ions resulting from the loss of guanidine that localize the site of dimethylation to the α-amine of Arg. Localization to Arg is further supported by loss of N^{α},N^{α}-dimethylArg (m/z 1180). **Denotes ions indicating that the sole azoline moiety of PZN is derived from the most C-terminal Thr residue. All masses are given in Da and represent the singly charged ion. For proposed structures of the daughter ions, see Supporting Figures S3 and S4.

clusters. We further demonstrate the *in vivo* biosynthesis of PZN in one of these newly identified producers.

Very recently, the structure of PZN from FZB42 was reported by Süssmuth and co-workers, primarily using 2D-NMR.[16] Independently, we employed mass spectrometry (MS) as our principle spectroscopic tool and arrived at the same structure. Through the use of high-resolution, linear ion trap Fourier transform hybrid MS (LTQ-FT) operating at 11 T, we measured the mass of the protonated form of PZN to be 1336.4783 Da (Figure 1a and Supporting Figure S1). Due to the high mass accuracy of FT-MS and the known sequence of the core region of the precursor peptide ($_1$RCTCTTIISSSSTF$_{14}$),[7,8] the molecular formula of [PZN + H]$^+$ can be deduced ($C_{63}H_{70}N_{17}O_{13}S_2$; theoretical monoisotopic mass = 1336.4780 Da; error, 0.22 ppm). This formula required that 9 out of 10 heterocyclizable residues (Cys, Ser, Thr) in the core region of the precursor peptide were converted to the azole heterocycle (Figure 1a). Due to their adjacent positions, these processed residues form a

contiguous polyazole, which was supported by spectrophotometric analysis. PZN gave absorption bands at 260 nm (λ_{max}), 310 nm (minor shoulder), and 370 nm (weak), indicating the presence of a complex chromophore (Supporting Figure S2). The remaining heterocyclizable residue was left at the azoline (thiazoline, oxazoline, or methyloxazoline) oxidation state. Also, this formula required leader peptide cleavage after Ala-Ala and two methylation events, consistent with earlier deletion studies.[8] Collision induced dissociation (CID) was then used to localize the site(s) of dimethylation and the azoline heterocycle. Analysis of the doubly charged PZN ion using in-line HPLC-FTMS resulted in a spectrum that was featureless from m/z ~700 to 1100 as a result of contiguous heterocycle formation (Supporting Figure S1). Nonetheless, we noted the production of several diagnostic fragment ions, including peptide bond cleavage at Ile-Ile. The masses of these resultant ions demonstrated that the N-terminal (b^+ ion) fragment contained both posttranslational methyl groups and that the C-terminal (y^+ ion) fragment contained the azoline (now restricted to oxazoline or methyloxazoline due to the absence of Cys on this fragment). Other informative fragment ions were derived from cleavage between Arg1-Cys2(thiazole) and Thr13(methyloxazoline)-Phe14. The former cleavage event demonstrated that both posttranslational methyl groups were localized to Arg1. Observation of the cleavage between Thre13-Phe12 and related decomposition products permitted the localization of the (methyl)oxazoline to Thr13. From the apparently unstable parent ion, we routinely observed formal loss of allene from methyloxazoline (C_3H_4, 40.0313 Da) to yield a C-terminal amide (Supporting Figure S1). Further support for the location of the azoline heterocycle comes from hydrolysis studies, as discussed below. Proposed structures for all assignable ions are given (Supporting Figures S3 and S4).

Upon in-depth FTMS analysis of singly charged PZN introduced by direct infusion, we observed larger ions relative to doubly charged PZN parent ions, including ones consistent with the loss of guanidine (−59.0483 Da, m/z 1277.4299; error, 0.63 ppm) (Figure 1b). This indicated that the site of dimethylation was restricted to either the N-terminal amine or the alkyl side chain of Arg1. The latter is exceedingly improbable since the enzyme known to catalyze this reaction (PznL) is predicted by sequence alignment to be a *S*-adenosylmethionine (SAM)-dependent methyltransferase. The only SAM-dependent enzymes capable of engaging in C−H bond activation are the radical SAM enzymes, which are identifiable by numerous conserved Cys lacking in PznL.[7,8,17] Higher order CID was performed on the deguanidinated form of PZN (m/z 1277), providing corroborating evidence for N-terminal dimethylation (Supporting Figure S5). Further support for the N-terminus being the site of dimethylation in PZN comes from chemoselective labeling. We reacted HPLC-purified PZN and desmethylPZN (from the *pznL* deletion strain) with the amine-specific reagent *N*-hydroxysuccinimide (NHS)-biotin.[8] As observed by MALDI-MS, labeling was only successful in the desmethylPZN reaction, indicating the presence of a free amine in this compound, but not in PZN (Supporting Figure S6). From these studies, we conclude that leader peptide cleavage occurs before methylation and that the ABC transport system does not distinguish between PZN and desmethylPZN. The nucleophilic N-terminus of desmethylPZN will likely be a convenient derivatization point for future structure−activity relationship (SAR) studies.

From the apparent hydrolysis of PZN following SDS-PAGE,[8] we were not surprised to find that PZN contained an azoline. Such heterocycles are prone to both acid- and base-catalyzed hydrolysis.[18,19] Mild acid treatment of PZN yields m/z 1354 (+18), which was shown by CID studies to be from the reconstitution of the Thr13 residue of the precursor peptide (Figure 1b). Higher order tandem MS experiments further confirmed the location of the PZN methyloxazoline moiety (Supporting Figures S4 and S5). Since the Thr13(methyloxazoline) is the only heterocycle not processed by the dehydrogenase, PznB displays a high level of regiospecificity. While our PZN structure is identical to that just published, note that Thr13 has been converted to a methyloxazoline, not a methyloxazolidine as reported.[16]

During our extensive MS analysis of PZN, we noticed that fragmentation of the methyloxazoline moiety gave rise to a characteristic mass loss. CID fragmentation of PZN yielded an intense daughter ion of m/z 1292.4519 (Figure 1b). The mass difference from the PZN parent ion is 44.0261 Da, which is consistent with the neutral loss of acetaldehyde (C_2H_4O, exact mass = 44.0262). Loss of acetaldehyde is conceivable from cycloelimination of methyloxazoline to yield a nitrile ylide, which can recyclize to form an azirine. The microscopic reverse of this reaction pathway is well-known in the chemical literature where azirines are reacted with aldehydes to form oxazolines *via* 1,3-dipolar cycloaddition.[18,20,21] Importantly, the loss of acetaldehyde was observed only when methyloxazoline was present on the parent ion (compare Figure 1b,c and Supporting Figures S3−S5). This observation could potentially be capitalized upon in future studies as a means of screening complex mixtures for the presence of azoline-bearing natural products.[3]

To corroborate the proposed structure elucidated by MS, we performed a series of two-dimensional NMR experiments including $^1H-^1H$-gCOSY, $^1H-^1H$-TOCSY, and $^1H-^{13}C$gHMBC on a 600 MHz instrument (Supporting Figures S7−S9). The results of these experiments are compiled in Supporting Table S1. Briefly, the gCOSY and TOCSY spectra confirmed the following: (i) Due to the absence of NH and $C_\alpha H$ correlations, all Cys, Ser, and Thr must be heterocyclized. The NH and $C_\alpha H$ correlations were readily visible for all internal residues with an intact amide bond (Ile, Ile, Phe). (ii) The carbon framework of the Arg1, Ile7, Ile8, and Phe14 side chains were not modified. (iii) The sole azoline moiety of PZN occurs on a Thr. The $^1H-^{13}C$-gHMBC spectrum further validated findings from the $^1H-^1H$ experiments, in addition to proving the methylation site as N^α, N^α-dimethylArg (Supporting Figure S9). N-Terminal methylation of ribosomally produced peptides in bacteria is an exceedingly rare posttranslational modification. While N-terminal dimethylation has been described on Ala (*e.g.*, cypemycin)[22] N^α,N^α-dimethylArg appears to be a novel posttranslational modification.[23] The structure of PZN provides yet another example of the complex natural product repertoire of *B. amyloliquefaciens* FZB42.[24]

During the course of optimizing the production of PZN for detailed spectroscopic analysis, we noticed that the level of culture oxygenation had a substantial impact on the production of PZN and derivative metabolites. Under low oxygen fermentation, PZN (m/z 1336) was the majority species present after a nonlytic, cell surface extraction procedure, as demonstrated by the UV trace, total ion chromatogram (TIC), and the extracted ion chromatogram (EIC, Figure 2a−c). The product of methyloxazoline ring opening (*i.e.*, hydrolyzed PZN, m/z 1354) was also

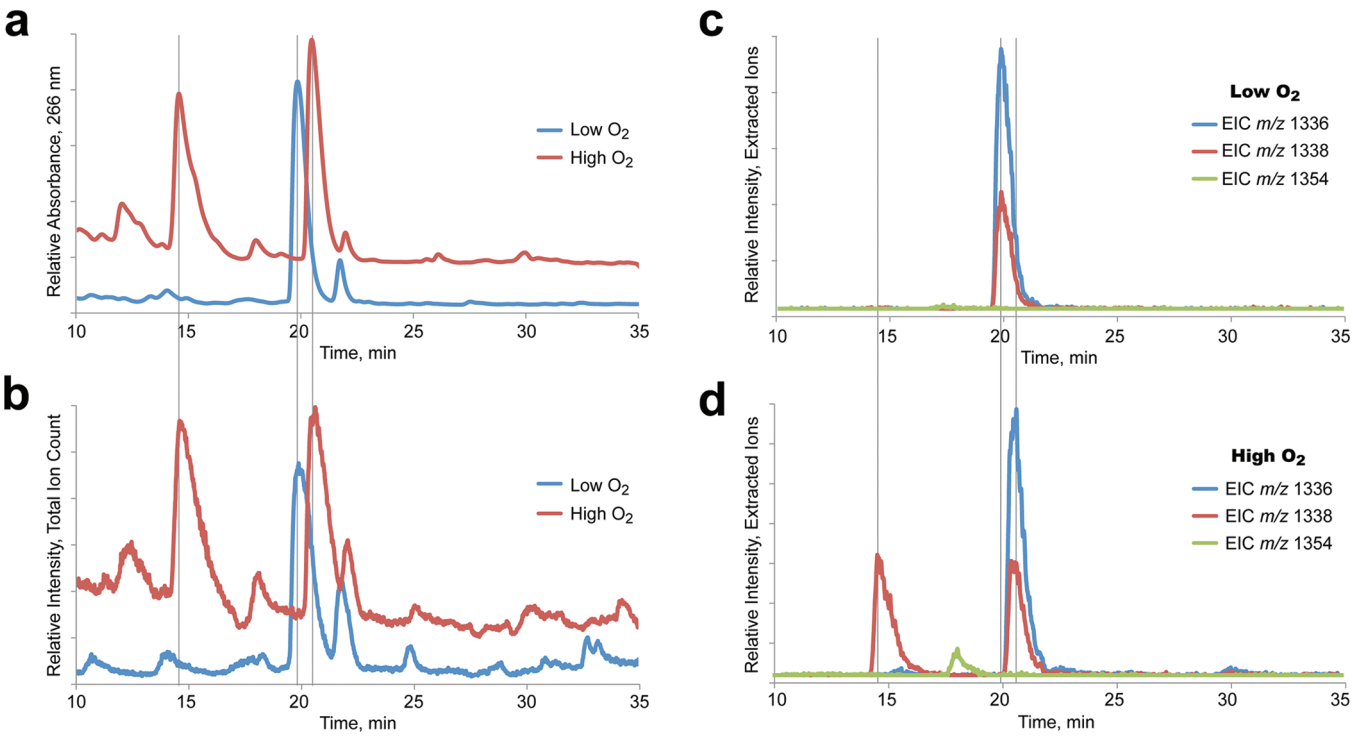

Figure 2. Effect of fermentation oxygenation on PZN production. High and low oxygenation cultures were extracted and subjected to chromatography using an identical procedure. In all panels, vertical lines were drawn at 14.7, 19.9, and 20.5 min. (a) UV chromatogram (abs 266 nm) of FZB42 strain RSpMarA2 extract from high and low oxygen fermentation. (b) Same as panel a except the trace is the total ion chromatogram (TIC). (c) Extracted ion chromatogram (EIC) of *m*/*z* 1336, 1338, and 1354 from a low oxygen fermentation. (d) Same as panel c except under high oxygenation conditions.

monitored (Figure 2c−d). The *m*/*z* 1338 species that "coelutes" with 1336 at 19.9 min is actually the second isotope peak of *m*/*z* 1336 (Supporting Figure S10). Under oxygen saturated cultivation, UV and TIC monitoring revealed an additional, highly abundant species at 14.7 min (Figure 2a,b). MS analysis demonstrated this species was *m*/*z* 1338, suggestive of a reduced PZN species (dihydroPZN) containing two azolines (Figure 2d, Supporting Figure S11). The earlier elution time on reverse-phase chromatography suggested that this species was more polar than PZN, which is consistent with the replacement of an aromatic azole with a protonated azoline (expected in 0.1% formic acid). After treatment of *m*/*z* 1338 with mild aqueous acid, two additions of water were observed (*m*/*z* 1356 and 1374). Tandem MS was then used to demonstrate that the second azoline was located on the N-terminal half of PZN (Supporting Figure S12). Higher order CID analysis prompted the neutral loss of acetaldehyde, indicating the heterocycle was derived from Thr, likely the residue directly preceding Ile (Thr6, data not shown). To an approximation, this position is sterically and electronically equivalent to the previously discussed methyloxazoline (Thr13) since both lie between an N-terminal tetra-azole and a C-terminal unmodified, hydrophobic residue (Figure 1a). The corresponding desmethylPZN species was observed when oxygenation levels were increased during cultivation of the methyltransferase deletion strain (Supporting Figures S13 and S14). It is possible that azoline oxidation is the rate-determining step in PZN biosynthesis. With increased aeration (faster metabolism), partially processed PZN products may be more rapidly produced and accepted as substrates by proteins acting downstream of the dehydrogenase. The biosynthetic implication of observing PZN oxidation intermediates is that the rate of methyloxazoline oxidation at "Thr6" (putative) and Thr13 (Figure 1a) must be slower than the dissociation rate from the heterotrimeric synthetase complex and subsequent maturation steps. An additional ramification of intercepting this PZN oxidation intermediate is that cyclodehydration must precede dehydrogenation, as has been previously supported by *in vitro* reconstitution experiments but never before demonstrated *in vivo*.[11,13] While the oxygen-dependency of secondary metabolism is well-known,[25] the precise mechanism accounting for the production of a more reduced PZN species during increased culture aeration is not clear at the present time.

In early 2011, the activity of PZN toward 16 distinct bacterial species (18 strains) was reported.[8] It was determined that PZN was growth-suppressive primarily toward *Bacillus* sp., including *B. subtilis*. PZN exhibited no activity against any tested Gram-negative organisms. To further define the selectivity within the Gram-positives, we evaluated the scope of PZN activity toward a panel of ubiquitous human pathogens, including methicillin-resistant *Staphylococcus aureus* (MRSA), vancomycin-resistant *Enterococcus faecalis* (VRE), *Listeria monocytogenes*, *Streptococcus pyogenes*, and *Bacillus anthracis* strain Sterne. Using a microbroth dilution bioassay, we observed potent growth inhibition of *B. anthracis* (Figure 3a). All other species were unaffected by PZN, with the exception of *S. pyogenes*, which was inhibited only by very high concentrations of PZN. The specificity for PZN against *B. anthracis* was recapitulated in an agar diffusion bioassay (Figure 3b), as inhibition zones were not observed for any other tested bacterium (data not shown). The action of PZN upon *B. anthracis* was decidedly bactericidal, as reculturing of treated cells in the absence of PZN led to no bacterial growth. Live cell imaging by differential interference contrast (DIC) microscopy

revealed that *B. anthracis* treated with PZN at 4 μg mL^{-1} underwent massive lysis, as evidenced by an abundance of cellular debris (data not shown). Of the few remaining nonlysed cells, we observed marked changes in the appearance of the cell surface (Figure 3c,d). While the biological target of PZN has yet to be established, the "sidewall spot" phenotype suggests PZN has either directly or indirectly compromised the integrity of the cell wall.[26] Due to the selective, biomedically relevant bactericidal activity exhibited by PZN, elucidation of the precise mode of action for PZN is ongoing in our laboratory.

a

Organism	MIC (μg/mL)	PZN variant	*B. anthracis* MIC (μg/mL)
B. anthracis	2-4	desmethylPZN	>128
E. faecalis (VRE)	>128	dihydroPZN*	>128
L. monocytogenes	>128	hydrolyzed PZN	32
S. aureus (MRSA)	>128		
S. pyogenes	128		

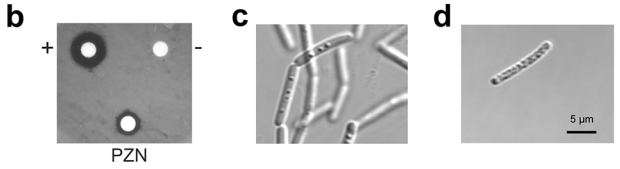

Figure 3. Assessment of PZN antibiotic activity. (a) The minimum inhibitory concentration (MIC) of HPLC-purified PZN was measured against a panel of Gram-positive human pathogens. Values reported were the concentration of PZN that inhibited 99% of bacterial growth in a microbroth dilution bioassay. *Due to separation difficulties, dihydroPZN was supplied as a 1:2:2 mixture of non-, mono-, and dihydrolyzed species (m/z 1338, 1356, 1374). (b) PZN activity in an agar disk diffusion bioassay against *B. anthracis* Sterne. Upper left disk, 8 μg of kanamycin control (positive); upper right, solvent control (negative); lower disk, 100 μg of PZN (200 μg gave a similar inhibition diameter). (c) Visual appearance of live *B. anthracis* Sterne treated with a solvent control by DIC microscopy. (d) Same as panel c, except cells were treated with 4 μg mL^{-1} PZN. Scale bar is the same for panel c.

Dimethylation of the α-amino group was apparently critical for PZN's antibiotic activity, as desmethylPZN was devoid of activity against *B. anthracis* in both bioassays (Figure 3a). While the molecular basis for this effect is not currently known, dimethylation increases amine basicity, lipophilicity, and removes two potential H-bond donors. Also tested were the effects of hydrolyzing the methyloxazoline moiety of PZN (hydrolyzed PZN, m/z 1354) and the variant with two azolines (dihydroPZN, m/z 1338). While hydrolyzed PZN retained measurable activity toward *B. anthracis*, dihydroPZN was devoid of activity. Due to difficulty in separating dihydroPZN from the mono- and dihydrolyzed forms (m/z 1356 and 1374), these bioassays were performed using a 1:2:2 mixture (non:mono:di). The lack of activity with this mixture of hydrolyzed, dihydroPZN compounds might be attributable to the fact that hydrolyzed PZN is roughly 8-fold less active than PZN (Figure 3a). Although the production of dihydroPZN under oxygen-saturated conditions may be artifactual, it nonetheless raises interesting questions regarding the regiospecificity of azoline oxidation and the substrate tolerance of the downstream tailoring enzymes and export apparatus.

A targeted bioinformatics survey using the thiazole/oxazole synthetase proteins (cyclodehydratase, dehydrogenase, and docking protein) of PZN yielded four highly related biosynthetic gene clusters (Figure 4). The cluster found in *Bacillus pumilus* ATCC 7061 (also a plant growth-promoting saprophyte) is of identical gene order and direction as the cluster from *B. amyloliquefaciens* FZB42.[8] The remaining three PZN-like biosynthetic clusters were found in the Actinobacteria phylum including *Clavibacter michiganensis* subsp. *sepedonicus* (potato pathogen),[27] *Corynebacterium urealyticum* DSM 7109 (human skin-associated bacterium, causative agent of some urinary tract infections), and *Brevibacterium linens* BL2 (human skin-associated bacterium). The PZN clusters from *C. urealyticum* and *B. linens* have amino acid similarity values much higher with each other than the other PZN producers, which is interesting given their overlapping niche and the absence of TOMM genes in sequenced relatives (Supporting Figure S15). In each of the five

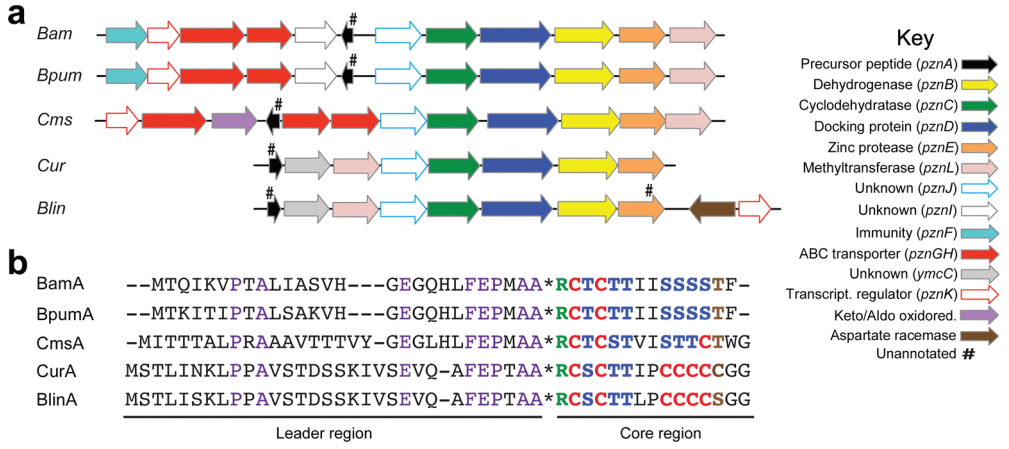

Figure 4. PZN biosynthetic gene clusters. (a) Open-reading frame diagram showing the genetic organization of PZN clusters, which form a subclass of TOMMs. Gene designations and predicted functions are color coded in the provided legend. (b) PZN precursor peptide alignment. Shown in purple are conserved residues within the N-terminal leader region. *Denotes the leader peptide cleavage site, which is known for BamA and BpumA but predicted for the others. Color-coding indicates the posttranslational modifications of the BamA core region, which are extrapolated to the remaining precursor peptides: N^{α},N^{α}-dimethylarginine (green), thiazoles (red), (methyl)oxazoles (blue), and methyloxazoline (brown). Abbreviations: Bam, *Bacillus amyloliquefaciens* FZB42; Bpum, *Bacillus pumilus* ATCC 7061; Cms, *Clavibacter michiganensis* subsp. *sepedonicus*; Cur, *Corynebacterium urealyticum* DSM 7109; Blin, *Brevibacterium linens* BL2.

dx.doi.org/10.1021/cb200339d |*ACS Chem. Biol.* 2011, 6, 1307–1313

species, the PZN biosynthetic cluster contained the canonical TOMM genes: a precursor peptide, dehydrogenase, cyclodehydratase, and docking protein. Beyond this, all five clusters also include a putative membrane-spanning leader peptidase from the type II CAAX superfamily,[28] SAM-dependent methyltransferase, and a required protein of unknown function.[8] Conversely, homologues of the PznF immunity protein and PznGH transporters were not found in the local genomic context for the PZN biosynthetic gene clusters for *C. urealyticum* and *B. linens* (Figure 4a). This suggests a distinct mechanism of immunity and chromosomally distant transporters for these PZN variants. Alternatively, the PZNs from *C. urealyticum* and *B. linens* could act intracellularly, or the biosynthetic gene cluster might always be silent (non-product forming).

On the basis of the identical amino acid sequence of the core regions of the precursor peptides from FZB42 and *B. pumilus*, it would be expected that these species produce identical compounds (Figure 4b). To test if *B. pumilus* was indeed producing PZN, stationary phase *B. pumilus* ATCC 7061 cultures were cell surface extracted in an identical manner as with FZB42. MALDI-TOF-MS of HPLC-purified fractions revealed the presence of m/z 1336 and, in an earlier fraction, m/z 1354 ($+H_2O$), supporting the production of PZN and hydrolyzed PZN (Supporting Figure S16a,b). The identity of this species as PZN was confirmed by high accuracy mass measurement (LTQ-FT-MS) and CID analysis (Supporting Figure S16c−e). As anticipated, *B. amylo*. FZB42 and *B. pumilus* were not susceptible to the action of PZN (MIC > 128 $\mu g\,mL^{-1}$). A non-plant-associated strain of *B. amylo*. (NRRL B-14393), which does not produce PZN, was also completely resistant (data not shown). Resistance within the *Bacillus* genus to PZN is clearly complex, with a few strains being *bona fide* PZN producers and others simply harboring the immunity gene [*e.g.*, *B. amylo*. strains YAU-Y2 and NAU-B3[8] and *B. atrophaeus* 1942, BATR1942_01200, 94% identical to FZB42]. Early attempts to isolate a PZN-type natural product from the Actinobacteria family members have not yet been successful. The lack of a signal by MALDI-MS and reverse transcriptase-PCR suggested that the biosynthetic genes were not transcribed under our cultivation conditions (data not shown). As with many "silent" gene clusters, highly precise environmental conditions are often necessary for the bacterium to produce particular natural products.

With several PZN-like biosynthetic gene clusters identified in this work, these natural products comprise an entirely new class of antibiotic. Sequence alignment of all five PZN precursor peptides showed that there has been evolutionary pressure to maintain a nearly invariant chemotype giving rise to the PZN structure (from N- to C-terminus): leader peptide cleavage site and N-terminal Arg (FEPxAA*R), five cyclizable residues with position 2 and 4 always Cys and position 6 always Thr, two hydrophobic residues, five cyclizable residues, and a more variable C-terminus that ends with Phe, Trp-Gly, or Gly-Gly (Figure 4b). It is probable that more PZN producers will emerge with ongoing efforts in genome sequencing. Future work will establish the contribution of these conserved functionalities on the bioactivity of PZN.

Here we have reported on the structural uniqueness of PZN, production of oxygen-dependent derivatives, distribution of producing species, and a striking human pathogen selectivity for *Bacillus anthracis*. Elucidation of the structure, in conjunction with the interception of dehydrogenase and methyltransferase intermediates, has provided a glimpse into the biosynthetic strategy employed by nature. With respect to the bioactivity of PZN, it is noteworthy that strains of *B. anthracis* have been reported to be increasingly resistant to the quinolone, β-lactam, tetracycline, and macrolide classes of antibiotics, and thus new strategies to overcome this NIAID-designated Category A priority pathogen are needed.[29,30] With improved diagnostic technology, we anticipate that highly discriminating antibiotics will play a large role in our future antibiotic repertoire. The ideal drugs will be capable of distinguishing between pathogenic bacteria and those that live in commensal and/or symbiotic relationships with humans. Selection theory predicts that such drugs will delay the rise of antibiotic resistance, as nontargeted species have no evolutionary benefit to develop/obtain a resistance mechanism. Faced with the never-ending arms race with multiple-drug-resistant bacteria, novel structural classes of antimicrobials with unique modes of action must continually be discovered and clinically implemented to treat bacterial infections. However, more work is necessary to determine if PZN-like compounds exhibit desirable *in vivo* properties.

■ ASSOCIATED CONTENT

Supporting Information. Methods and additional spectroscopic and chromatographic data of PZN and variants; bioinformatic and production data on alternate producers of PZN. This material is available free of charge *via* the Internet at http://pubs.acs.org.

■ AUTHOR INFORMATION

Corresponding Author
*E-mail: douglasm@illinois.edu.

■ DISCLOSURE

The authors declare that they have no conflict of interest.

■ ACKNOWLEDGMENT

We are grateful for the gift of *B. amyloliquefaciens* strains RSpMarA2 and RS33 from R. Borriss (Humboldt Universität Berlin, Germany). VRE strain U503 and *S. aureus* strain NRS-384/USA300 were kindly provided by J. Williams and P. Hergenrother (University of Illinois), and *L. monocytogenes* and *B. anthracis* Sterne were from J. Call (USDA-ARS) and S. Stibitz (FDA), respectively. T. Maxson, N. Ethridge, A. Mohan, and M. Sivaguru are acknowledged for their technical assistance. Members of the Mitchell lab assisted in the critical review of this manuscript. This work was supported by institutional funds provided by the University of Illinois (D.A.M.) and the NIH (GM 067193, N.L.K.). K.J.M. was supported in part by a Graduate College Fellowship (University of Illinois) and NIH Cellular and Molecular Biology Training Grant (T32 GM007-283). K.L.D. was supported by the NIH Training Program in Chemistry−Interface with Biology (T32 GM070421).

■ REFERENCES

(1) Challis, G. L. (2008) Genome mining for novel natural product discovery. *J. Med. Chem. 51*, 2618–2628.

(2) Gross, H. (2009) Genomic mining—a concept for the discovery of new bioactive natural products. *Curr. Opin. Drug Discovery Dev. 12*, 207–219.

(3) Melby, J. O., Nard, N. J., and Mitchell, D. A. (2011) Thiazole/oxazole-modified microcins: complex natural products from ribosomal templates. *Curr. Opin. Chem. Biol. 15*, 369–378.
(4) Peric-Concha, N., and Long, P. F. (2003) Mining the microbial metabolome: a new frontier for natural product lead discovery. *Drug Discovery Today 8*, 1078–1084.
(5) Newman, D. J., and Cragg, G. M. (2007) Natural products as sources of new drugs over the last 25 years. *J. Nat. Prod. 70*, 461–477.
(6) Haft, D. H., Basu, M. K., and Mitchell, D. A. (2010) Expansion of ribosomally produced natural products: a nitrile hydratase- and Nif11-related precursor family. *BMC Biol. 8*, 70.
(7) Lee, S. W., Mitchell, D. A., Markley, A. L., Hensler, M. E., Gonzalez, D., Wohlrab, A., Dorrestein, P. C., Nizet, V., and Dixon, J. E. (2008) Discovery of a widely distributed toxin biosynthetic gene cluster. *Proc. Natl. Acad. Sci. U.S.A. 105*, 5879–5884.
(8) Scholz, R., Molohon, K. J., Nachtigall, J., Vater, J., Markley, A. L., Sussmuth, R. D., Mitchell, D. A., and Borriss, R. (2011) Plantazolicin, a novel microcin B17/streptolysin S-like natural product from *Bacillus amyloliquefaciens* FZB42. *J. Bacteriol. 193*, 215–224.
(9) Madison, L. L., Vivas, E. I., Li, Y. M., Walsh, C. T., and Kolter, R. (1997) The leader peptide is essential for the post-translational modification of the DNA-gyrase inhibitor microcin B17. *Mol. Microbiol. 23*, 161–168.
(10) Mitchell, D. A., Lee, S. W., Pence, M. A., Markley, A. L., Limm, J. D., Nizet, V., and Dixon, J. E. (2009) Structural and functional dissection of the heterocyclic peptide cytotoxin streptolysin S. *J. Biol. Chem. 284*, 13004–13012.
(11) McIntosh, J. A., and Schmidt, E. W. (2010) Marine molecular machines: heterocyclization in cyanobactin biosynthesis. *ChemBioChem 11*, 1413–1421.
(12) Milne, J. C., Eliot, A. C., Kelleher, N. L., and Walsh, C. T. (1998) ATP/GTP hydrolysis is required for oxazole and thiazole biosynthesis in the peptide antibiotic microcin B17. *Biochemistry 37*, 13250–13261.
(13) Milne, J. C., Roy, R. S., Eliot, A. C., Kelleher, N. L., Wokhlu, A., Nickels, B., and Walsh, C. T. (1999) Cofactor requirements and reconstitution of microcin B17 synthetase: a multienzyme complex that catalyzes the formation of oxazoles and thiazoles in the antibiotic microcin B17. *Biochemistry 38*, 4768–4781.
(14) Donia, M. S., Ravel, J., and Schmidt, E. W. (2008) A global assembly line for cyanobactins. *Nat. Chem. Biol. 4*, 341–343.
(15) Wieland Brown, L. C., Acker, M. G., Clardy, J., Walsh, C. T., and Fischbach, M. A. (2009) Thirteen posttranslational modifications convert a 14-residue peptide into the antibiotic thiocillin. *Proc. Natl. Acad. Sci. U.S.A. 106*, 2549–2553.
(16) Kalyon, B., Helaly, S. E., Scholz, R., Nachtigall, J., Vater, J., Borriss, R., and Sussmuth, R. D. (2011) Plantazolicin A and B: structure elucidation of ribosomally synthesized thiazole/oxazole peptides from *Bacillus amyloliquefaciens* FZB42. *Org. Lett. 13*, 2996–2999.
(17) Frey, P. A., Hegeman, A. D., and Ruzicka, F. J. (2008) The radical SAM superfamily. *Crit. Rev. Biochem. Mol. Biol. 43*, 63–88.
(18) Frump, J. A. (1971) Oxazolines. Their preparation, reactions, and applications. *Chem Rev 71*, 483–505.
(19) Martin, R. B., and Parcell, A. (1961) Hydrolysis of 2-methyl-delta-oxazoline—an intramolecular O-N-acetyl transfer reaction. *J. Am. Chem. Soc. 83*, 4835–4838.
(20) Giezenda, H., Heimgart, H., Jackson, B., Winkler, T., Hansen, H. J., and Schmid, H. (1973) Photoreactions 0.31. Photochemical cycloadditions of 3-phenyl-2H-azirines with aldehydes. *Helv. Chim. Acta 56*, 2611–2627.
(21) Sa, M. C. M., and Kascheres, A. (1996) Electronically mediated selectivity in ring opening of 1-azirines. The 3-X mode: Convenient route to 3-oxazolines. *J. Org. Chem. 61*, 3749–3752.
(22) Claesen, J., and Bibb, M. (2010) Genome mining and genetic analysis of cypemycin biosynthesis reveal an unusual class of posttranslationally modified peptides. *Proc. Natl. Acad. Sci. U.S.A. 107*, 16297–16302.
(23) Garavelli, J. S. (2004) The RESID Database of Protein Modifications as a resource and annotation tool. *Proteomics 4*, 1527–1533.
(24) Chen, X. H., Koumoutsi, A., Scholz, R., Eisenreich, A., Schneider, K., Heinemeyer, I., Morgenstern, B., Voss, B., Hess, W. R., Reva, O., Junge, H., Voigt, B., Jungblut, P. R., Vater, J., Sussmuth, R., Liesegang, H., Strittmatter, A., Gottschalk, G., and Borriss, R. (2007) Comparative analysis of the complete genome sequence of the plant growth-promoting bacterium *Bacillus amyloliquefaciens* FZB42. *Nat. Biotechnol. 25*, 1007–1014.
(25) Clark, G. J., Langley, D., and Bushell, M. E. (1995) Oxygen limitation can induce microbial secondary metabolite formation—investigations with miniature electrodes in shaker and bioreactor culture. *Microbiology (Reading, U. K.) 141*, 663–669.
(26) Tiyanont, K., Doan, T., Lazarus, M. B., Fang, X., Rudner, D. Z., and Walker, S. (2006) Imaging peptidoglycan biosynthesis in *Bacillus subtilis* with fluorescent antibiotics. *Proc. Natl. Acad. Sci. U.S.A. 103*, 11033–11038.
(27) Bentley, S. D., Corton, C., Brown, S. E., Barron, A., Clark, L., Doggett, J., Harris, B., Ormond, D., Quail, M. A., May, G., Francis, D., Knudson, D., Parkhill, J., and Ishimaru, C. A. (2008) Genome of the actinomycete plant pathogen *Clavibacter michiganensis* subsp. sepedonicus suggests recent niche adaptation. *J. Bacteriol. 190*, 2150–2160.
(28) Pei, J., Mitchell, D. A., Dixon, J. E., and Grishin, N. V. (2011) Expansion of type II CAAX proteases reveals evolutionary origin of γ-secretase subunit APH-1. *J. Mol. Biol. 410*, 18–26.
(29) Athamna, A., Athamna, M., Abu-Rashed, N., Medlej, B., Bast, D. J., and Rubinstein, E. (2004) Selection of *Bacillus anthracis* isolates resistant to antibiotics. *J. Antimicrob. Chemother. 54*, 424–428.
(30) Bryskier, A. (2002) *Bacillus anthracis* and antibacterial agents. *Clin. Microbiol. Infect. 8*, 467–478.